Title
Global and regional brain mean diffusivity changes in patients with heart failure.

Journal
Journal of neuroscience research, 93(4)

ISSN
0360-4012

Authors
Woo, Mary A
Palomares, Jose A
Macey, Paul M
et al.

Publication Date
2015-04-01

DOI
10.1002/jnr.23525

Peer reviewed

Journal of Neuroscience Research 93:678–685 (2015)

Global and Regional Brain Mean Diffusivity Changes in Patients With Heart Failure

Mary A. Woo,[1] Jose A. Palomares,[2] Paul M. Macey,[1,3] Gregg C. Fonarow,[4] Ronald M. Harper,[3,5] and Rajesh Kumar[2,3,6,7]*

[1]UCLA School of Nursing, University of California at Los Angeles, Los Angeles, California
[2]Department of Anesthesiology, University of California at Los Angeles, Los Angeles, California
[3]Brain Research Institute, University of California at Los Angeles, Los Angeles, California
[4]Division of Cardiology, University of California at Los Angeles, Los Angeles, California
[5]Department of Neurobiology, University of California at Los Angeles, Los Angeles, California
[6]Department of Radiological Sciences, University of California at Los Angeles, Los Angeles, California
[7]Department of Bioengineering, University of California at Los Angeles, Los Angeles, California

Heart failure (HF) patients show gray and white matter changes in multiple brain sites, including autonomic and motor coordination areas. It is unclear whether the changes represent acute or chronic tissue pathology, a distinction necessary for understanding pathological processes that can be resolved with diffusion tensor imaging (DTI)-based mean diffusivity (MD) procedures. We collected four DTI series from 16 HF (age 55.1 ± 7.8 years, 12 male) and 26 control (49.7 ± 10.8 years, 17 male) subjects with a 3.0-Tesla magnetic resonance imaging scanner. MD maps were realigned, averaged, normalized, and smoothed. Global and regional MD values from autonomic and motor coordination sites were calculated by using normalized MD maps and brain masks; group MD values and whole-brain smoothed MD maps were compared by analysis of covariance (covariates; age and gender). Global brain MD (HF vs. controls, units × 10^{-6} mm^2/sec, 1103.8 ± 76.6 vs. 1035.9 ± 69.4, $P = 0.038$) and regional autonomic and motor control site values (left insula, 1,085.4 ± 95.7 vs. 975.7 ± 65.4, $P = 0.001$; right insula, 1,050.2 ± 100.6 vs. 965.7 ± 58.4, $P = 0.004$; left hypothalamus, 1,419.6 ± 165.2 vs. 1,234.9 ± 136.3, $P = 0.002$; right hypothalamus, 1,446.5 ± 178.8 vs. 1,273.3 ± 136.9, $P = 0.004$; left cerebellar cortex, 889.1 ± 81.9 vs. 796.6 ± 46.8, $P < 0.001$; right cerebellar cortex, 797.8 ± 50.8 vs. 750.3 ± 27.5, $P = 0.001$; cerebellar deep nuclei, 1,236.1 ± 193.8 vs. 1,071.7 ± 107.1, $P = 0.002$) were significantly higher in HF vs. control subjects, indicating chronic tissue changes. Whole-brain comparisons showed increased MD values in HF subjects, including limbic, basal-ganglia, thalamic, solitary tract nucleus, frontal, and cerebellar regions. Brain injury occurs in autonomic and motor control areas, which may contribute to deficient function in HF patients. The chronic tissue changes likely result from processes that develop over a prolonged period.

Key words: autonomic; insula cerebellum; chronic injury; diffusion tensor imaging; dyspnea

Heart failure (HF) patients show gray matter and axonal deficits in multiple autonomic, motor, cognitive, and emotional regulatory brain areas (Woo et al., 2003, 2009; Kumar et al., 2009, 2011). The nature of brain structural deficits is unclear; specifically, it is unknown whether the pathology results from transient or catastrophic events in close temporal relationship to recognition of the damage or whether the injury develops from processes requiring substantial time periods to emerge. Determining the developmental course of pathology in HF is essential for understanding the ongoing injurious processes, which would help guide intervention strategies for neural protection in the condition.

Noninvasive magnetic resonance imaging (MRI) procedures can differentiate whether structural changes result from acute or chronic processes (Matsumoto et al., 1995; Ahlhelm et al., 2002). Diffusion tensor imaging (DTI)-based mean diffusivity (MD) is a measure of average water diffusion within tissue and can show changes in tissue integrity, an index that is affected by extracellular/intracellular water content and tissue barriers, including cellular and axonal membranes and macromolecules (Basser and Pierpaoli, 1996; Le Bihan et al., 2001). The procedures show differential values in various pathological stages, with decreased MD values appearing in acute conditions and increased MD values materializing in chronic injury (Matsumoto et al., 1995; Ahlhelm et al., 2002).

Contract grant sponsor: NIH; Contract grant number: R01 NR-013625; Contract grant number: R01 NR-014669.

*Correspondence to: Rajesh Kumar, PhD, Department of Anesthesiology, David Geffen School of Medicine at UCLA, 56-132 CHS, 10833 Le Conte Ave, University of California at Los Angeles, Los Angeles, CA 90095-1763. E-mail: rkumar@mednet.ucla.edu

Received 7 September 2014; Revised 28 October 2014; Accepted 30 October 2014

Published online 13 December 2014 in Wiley Online Library (wileyonlinelibrary.com). DOI: 10.1002/jnr.23525

TABLE I. Demographic, Biophysical, and Clinical Data From HF and Control Subjects

Variables	HF (n = 16)	Controls (n = 26)	*P* values
Age (years)	55.1 ± 7.8	49.7 ± 10.8	0.07
Gender (male:female)	12:4	17:9	0.43
Body Mass Index (kg/m^2)	29.6 ± 5.8	26.4 ± 4.3	0.07
LVEF* (%)	27.7 ± 6.7	—	—
HF diagnosis	NYHA functional class II	—	—
Handedness	Right, 15; left, 1	Right, 21; left, 3; both, 2	—
Ethnicity	White, 10; African-American, 2; Hispanic, 1; Asian, 1; other, 2	White, 18; Hispanic, 4; Asian, 4	—

*LVEF, left ventricular ejection fraction.

The MD procedures have been used in various pathological conditions to characterize tissue damage and may provide insights into altered states of brain tissue in HF patients (Matsumoto et al., 1995; Ahlhelm et al., 2002).

This study examines global and regional brain tissue changes by using DTI-based MD procedures in HF and control subjects to determine whether the structural changes result from acute or chronic processes. We hypothesized that, based on the severity and duration of autonomic changes exhibited by these patients, both global and regional brain MD values, including autonomic and motor regulatory sites, would be increased in HF compared with control subjects, reflecting chronic tissue changes in the condition.

MATERIALS AND METHODS

Sixteen hemodynamically optimized HF and 26 healthy control subjects were studied. Demographic, biophysical, and clinical variables of HF and control subjects are summarized in Table I. All HF subjects were diagnosed based on national HF diagnostic criteria (Radford et al., 2005), showed dilated cardiomyopathy and systolic dysfunction, were classified as New York Heart Association (NYHA) functional class III–IV but included only NYHA functional class II subjects after HF treatment at the time of MRI, and were recruited from the Ahmanson-UCLA Cardiomyopathy Center. HF patients with NYHA III and IV were excluded for logistic reasons because HF patients with such classifications cannot lay supine in the MRI scanner for a long period. We performed brain MRI on subjects within 1 year of HF diagnosis to minimize variability in measures from disease onset. All HF subjects were hemodynamically optimized before MRI and underwent similar treatment and care. HF subjects had no previous history of stroke or carotid vascular disease and were treated with angiotensin-converting enzyme inhibitors or angiotensin receptor blockers, diuretics, and beta blockers titrated to specific hemodynamic goals. All control subjects were recruited from the UCLA Medical Center and West Los Angeles area through flyers and postings. All control subjects were healthy and were screened for head injury; history of cardiovascular, cerebrovascular, respiratory, or neurological disorders; and use of cardiac or psychotropic medications that might introduce brain changes. None of the controls included in this study were taking any such medications, and all denied acute head injury or any potential chronic injury (e.g., football or hockey injury). Control subjects were interviewed for the presence of obstructive sleep apnea, and suspected subjects underwent an overnight sleep study. Neither HF nor control subjects had metallic implants; all had body weights less than 125 kg and no conditions contraindicated for an MRI scanner environment. All HF and control subjects gave written informed consent before the study, and the study protocol was approved by the Institutional Review Board of the University of California at Los Angeles.

MRI

Brain imaging of HF and control subjects was performed with a 3.0-Tesla MRI scanner (Magnetom Tim-Trio; Siemens, Erlangen, Germany) with an eight-channel phased-array head coil. Foam pads were placed on both sides of the head to minimize head motion-related artifacts. High-resolution T1-weighted images were acquired by using a magnetization-prepared rapid acquisition gradient-echo pulse sequence (repetition time [TR] = 2,200 msec; echo time [TE] = 2.2 msec; inversion time = 900 msec; flip angle [FA] = 9°; matrix size = 256 × 256; field of view [FOV] = 230 × 230 mm; slice thickness = 1.0 mm). Proton density (PD) and T2-weighted images were collected simultaneously in the axial plane by using a dual-echo turbo spin-echo pulse sequence (TR = 10,000 msec; TE1, 2 = 17, 134 msec; FA = 130°; matrix size = 256 × 256; FOV = 230 × 230 mm; slice thickness = 4.0 mm). DTI was performed by using single-shot echo-planar imaging with twice-refocused spin-echo pulse sequence (TR = 10,000 msec; TE = 87 msec; FA = 90°; bandwidth = 1,346 Hz/pixel; matrix size = 128 × 128; FOV = 230 × 230 mm; slice thickness = 2.0 mm, no interslice gap, diffusion values = 0 and 700 sec/mm^2; diffusion gradient directions = 12; separate series = 4). The parallel imaging technique, generalized autocalibrating partially parallel acquisition with an acceleration factor of 2, was used in high-resolution T1-weighted, PD-weighted, T2-weighted, and DTI data acquisition.

Data Processing and Analysis

The statistical parametric mapping package SPM8 (http://www.fil.ion.ucl.ac.uk/spm/), DTI-Studio (v3.0.1; Jiang et al., 2006), MRIcroN (Rorden et al., 2007), and MATLAB-based (http://www.mathworks.com/) custom software were used for evaluation of images, data processing, and analyses. High-resolution T1-weighted, PD-weighted, and T2-weighted images of HF and control subjects were evaluated for any visible brain pathology, including tumors, cysts, or any other mass lesions. Diffusion- and nondiffusion-weighted images of HF and control

TABLE II. Global and Regional Brain MD Values of HF and Control Subjects⋆

Brain sites	HF (n = 16)	Controls (n = 26)	*P* values	*P* values‡
Global brain	1,103.8 ± 76.6	1,036.0 ± 69.4	0.005	0.038
Left insula	1,085.4 ± 95.7	975.7 ± 65.4	< 0.001	0.001
Right insula	1,050.2 ± 100.6	965.8 ± 58.4	0.001	0.004
Left hypothalamus	1,419.7 ± 165.2	1,234.9 ± 136.3	< 0.001	0.002
Right hypothalamus	1,446.5 ± 178.8	1,273.3 ± 136.9	0.003†	0.004
Left cerebellar cortex	889.1 ± 81.9	796.6 ± 46.8	<0.001	< 0.001
Right cerebellar cortex	797.9 ± 50.8	750.4 ± 27.5	<0.001†	0.001
Cerebellar deep nuclei	1,236.1 ± 193.8	1,071.7 ± 107.7	0.005†	0.002

⋆Mean ± SD; unit, 10^{-6} mm^2/sec.
†Equal variances not assumed.
‡*P* values based on analysis of covariance (covariates are age and gender).

subjects for imaging or head motion-related artifacts were examined before MD quantification. Neither HF nor control subjects showed major visible brain tissue changes or head-motion or other imaging artifacts.

Calculation of MD maps. The average background noise level from outside the brain tissue was derived by using nondiffusion- and diffusion-weighted images; this noise threshold was used in all subjects to suppress noise outside the brain parenchyma during MD calculations. By using diffusion-weighted (b = 700 sec/mm^2) and nondiffusion-weighted (b = 0 sec/mm^2) images, diffusion tensors were calculated in DTI-Studio software (Jiang et al., 2006), and principal eigenvalues ($\lambda1$, $\lambda2$, and $\lambda3$) were derived by diagonalizing the diffusion tensor matrices (Basser and Pierpaoli, 1996, 1998). By using principal eigenvalues, MD maps ($MD = [\lambda1 + \lambda2 + \lambda3]/3$) were derived from each DTI series (Basser and Pierpaoli, 1996; Le Bihan et al., 2001).

MD maps: realignment, averaging, normalization, and smoothing. Four MD maps, derived from each separate DTI series, were realigned to remove any possible misalignment resulting from head motion and averaged. Similarly, nondiffusion-weighted images (b0 images) from each DTI series were realigned and averaged.

The averaged MD maps of all HF and control subjects were normalized to Montreal Neurological Institute (MNI) common space. Based on a priori defined distributions of gray, white, and cerebrospinal fluid tissue types (Ashburner and Friston, 2005), the averaged nondiffusion-weighted images were normalized to MNI space, and the resulting normalization parameters were applied to the corresponding subject's MD and tissue probability maps and nondiffusion-weighted images. An isotropic Gaussian filter (10-mm kernel) was used to smooth the normalized MD maps. We also normalized high-resolution T1-weighted images of HF and control subjects to MNI space; these images were averaged to derive a whole-brain mean background image for structural identification.

Global brain mask. The normalized gray matter probability maps were averaged from all HF and control subjects. Similarly, the normalized white matter probability maps from HF and control subjects were averaged. The averaged gray and white matter probability maps were thresholded (white matter probability > 0.3, gray matter probability > 0.3), and both thresholded probability maps were combined to create one global brain mask.

Calculation of global brain MD values. The normalized MD maps of HF and control subjects were masked by using a global brain mask to remove nonbrain regions. The masked MD maps of individuals were used to derive mean global brain MD values in MATLAB-based custom software.

Region of interest analyses. Region of interest analyses were performed to determine regional MD values, including the insular cortices, hypothalamus, and cerebellar cortices and deep nuclei from HF and control subjects. Regional brain masks were created based on significant whole-brain voxel-by-voxel differences between groups for those regions, and values were extracted by using these regional brain masks and normalized MD maps of HF and control subjects.

Statistical Analysis

SPSS v22 (IBM, Armonk, NY) software was used to examine demographic and biophysical variables and global and regional brain mean MD values. Independent-samples *t*-tests and χ^2 were used to examine the demographic and biophysical variables. The global and regional brain MD values were examined for significant differences between HF and control subjects by analysis of covariance (ANCOVA), with age and gender included as covariates. $P < 0.05$ was considered statistically significant. Regional brain differences between male and female control subjects have been well described (Menzler et al., 2011; Westerhausen et al., 2011); the odd ratio of sex in both groups mandated factoring gender as another covariate in the statistical model.

The normalized and smoothed MD maps were compared voxel by voxel between HF and control subjects by ANCOVA, with age and gender included as covariates (SPM8, uncorrected threshold, $P < 0.005$; minimum extended cluster size five voxels). An arbitrary extended cluster size (five voxels) was used to avoid brain areas showing unreliable significant differences between groups (Kumar et al., 2011). Brain clusters were overlaid with significant differences between groups onto background images for structural identification.

RESULTS

Demographic, Biophysical, and Clinical Variables

Demographic, biophysical, and clinical data of HF and control subjects are summarized in Table I. HF subjects did not differ significantly in age, gender, or body mass index from control subjects.

Global and Regional MD Values

Global and regional brain MD values of HF and control subjects are tabulated in Table II. Mean global brain MD values were significantly increased in HF compared with control subjects, and, similarly, regional autonomic and motor regulatory sites showed higher MD values in HF vs. control subjects (Table II).

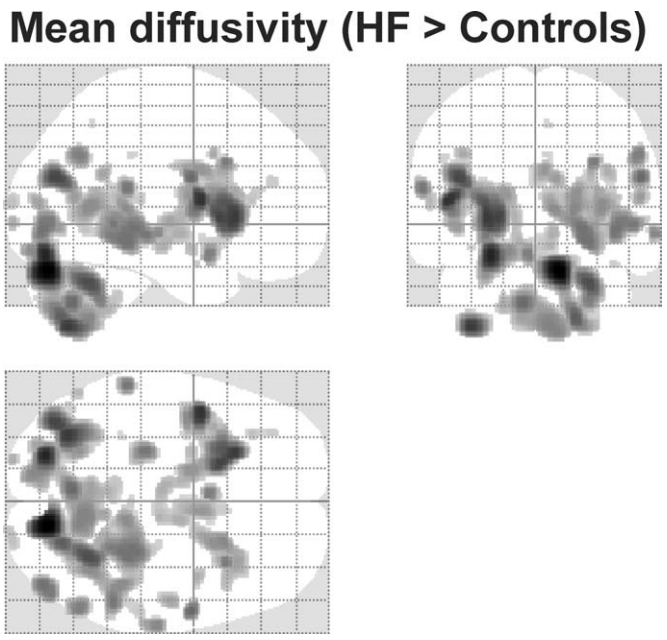

Fig. 1. Brain regions with significantly increased MD values in HF (n = 16) vs. healthy control (n = 26) subjects (uncorrected threshold, $P = 0.005$) are shown in glass brain format with projections across the 3D onto the 2D axial, sagittal, and coronal views.

Whole-Brain MD Changes

Multiple brain sites in HF subjects showed significantly increased MD values vs. control subjects (Fig. 1), including the frontal white matter (Fig. 2a), external and internal capsules (Fig. 2b,i), ventral hippocampus (Fig. 2c), cerebellar cortices (Figs. 2d, 3d,e), parietal cortices (Fig. 2e), and mid- and posterior cingulate cortices (Fig. 2f,g) extending to corpus callosum (Figs. 2n,p, 3f,g), septum/bed nuclei (Fig. 2j), putamen (Fig. 2k), insular cortices (Fig. 2l), caudate nuclei (Fig. 2m), ventral white matter (Fig. 2o), anterior and posterior thalamus (Figs. 2q,r, 3j), and occipital gray and white matter (Fig. 2h,s). Other sites with increased MD values in HF vs. control subjects included the genu of cingulate (Fig. 3a) extending to hypothalamus (Fig. 3b), ventrolateral tegmental area (Fig. 3c), cerebellar vermis (Fig. 3e), raphe extending to nucleus of the solitary tract (NTS; Fig. 3h), inferior cerebellar peduncles (Fig. 3k), and cerebellar deep nuclei (Fig. 3i).

DISCUSSION

Overview

HF subjects showed increased MD values relative to control subjects over the entire brain and in specific brain regions; increased MD values normally reflect chronic tissue changes. Regional tissue damage typically appeared in autonomic and motor control sites, including the insular cortices, hypothalamus, and cerebellar cortices and deep nuclei. Other brain regions with damage included the limbic, basal ganglia, thalamic, NTS, and frontal areas. The injury in these brain sites emerged in our earlier studies either as structural tissue changes or as functional deficits and was determined by various structural and functional MRI procedures during autonomic challenges (Woo et al., 2003, 2005, 2009). The long-term brain changes may result from multiple pathological processes, but ischemia and hypoxia accompanying the condition likely contribute.

Acute and Chronic Tissue Changes and MD Values

Noninvasive DTI-based MD procedures can be used to examine global and regional brain tissue integrity. MD values can be altered by several factors, including tissue barriers (Le Bihan et al., 1991), water content, and extracellular/axonal space. Acute hypoxia or ischemia establishes a sequence of energy pump failure, altering sodium, potassium, and calcium ionic flow, leading to cytotoxic edema, with cytotoxic processes decreasing extracellular/axonal water and introducing neuronal and axonal swelling (Hossmann, 1971; O'Dell et al., 1994; Dirnagl et al., 1999). Such changes lead to restricted water diffusion within tissue, resulting in reduced MD values (Matsumoto et al., 1995; Ahlhelm et al., 2002). However, chronic stages of hypoxia or ischemia result in degeneration of neurons and axons, which allow more extracellular/axonal water content and increased space, permitting water molecules to move faster within tissue, leading to increased regional MD values (Matsumoto et al., 1995; Ahlhelm et al., 2002).

Because HF subjects showed global and regional increased MD values, the processes found here likely result from chronic pathological mechanisms. Chronic tissue changes may require a variable period of time to develop, ranging from a week to years, depending on the extent of hypoxic/ischemic stress. The history of our subjects suggests that pathological processes had been operating for several years.

Autonomic, Respiratory, and Motor Regulatory Sites and Brain Changes

Multiple autonomic and motor control sites, including the insular and cingulate cortices, hypothalamus, NTS, cerebellar cortices, vermis, and deep nuclei, showed increased MD values, indicating tissue injury in these areas in HF vs. control subjects. Left and right insular cortices have different autonomic control roles along with other affective and pain-regulatory functions. Both human and animal studies indicate that the right insula is involved primarily in sympathetic modulation and the left insula is involved primarily in parasympathetic regulation (Cechetto and Saper, 1987; Oppenheimer et al., 1992, 1996; Zhang et al., 1998); both insular cortices play numerous other sensory integration roles (Shipley, 1982; Cechetto and Chen, 1990; Oppenheimer et al., 1992). Insular cortices receive visceral sensory input from, and project to, the hypothalamus, participating significantly in autonomic regulation (Saper, 1982; Oppenheimer et al., 1996). Other major contributors to autonomic regulation,

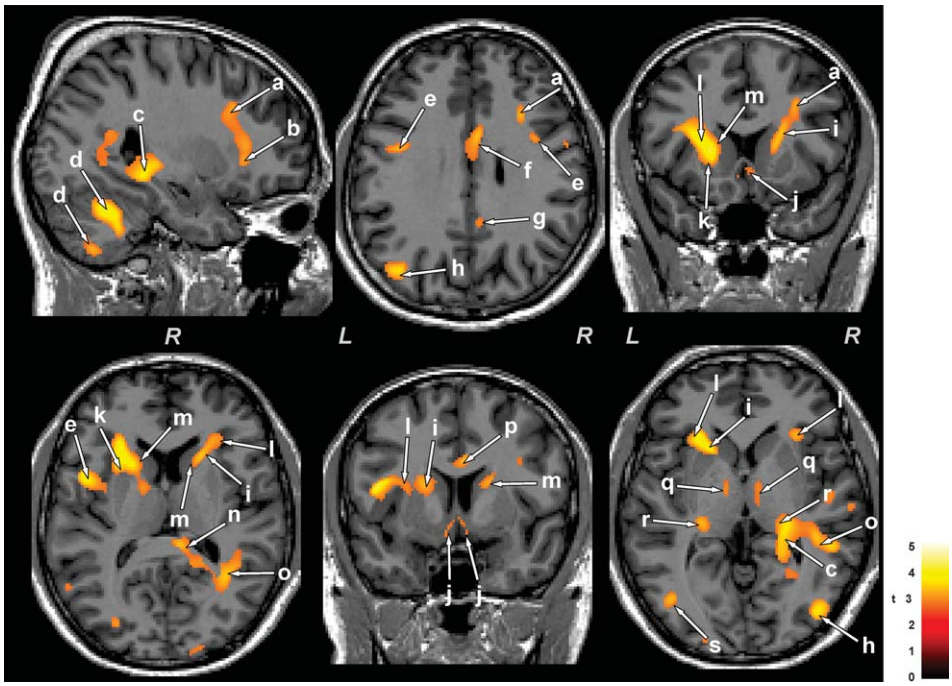

Fig. 2. Brain sites with significantly increased MD values in HF vs. control subjects. Significantly increased MD values in HF subjects appeared in brain sites, including the frontal white matter (a), external and internal capsules (b,i), ventral hippocampus (c), cerebellar cortices (d), parietal cortices (e), mid- and posterior cingulate cortices (f,g), occipital gray and white matter (h,s), septum/bed nuclei (j), putamen (k), insular cortices (l), caudate nuclei (m), posterior corpus callosum (n,p), ventral white matter (o), and anterior and posterior thalamus (q,r). All brain images are in neurological convention (L = left, R = right), and the color scale shows *t*-statistic values.

the cingulate and the ventral medial prefrontal cortices (King et al., 1999; Critchley et al., 2003), also project to the insular cortices, and the mid- and posterior cingulate cortices showed injury here. HF patients show both long-lasting increased sympathetic and altered parasympathetic tone (Woo et al., 2005), and the insular and cingulate cortices and hypothalamic chronic tissue injury found here likely contributed to those altered autonomic aspects in the syndrome, as shown by distorted functional MRI signal responses in HF subjects to autonomic challenges, including the Valsalva maneuver and cold pressor (Woo et al., 2005, 2007).

The NTS and raphe projections assist cardiovascular regulatory processes that include baroreceptor and chemoreceptor reflexes, failure of which results in essential features that characterize the pathology of HF (Kumar et al., 2011). The NTS serves such a critical role in coordination of blood pressure and chemoreception that any injury to that structure would severely disrupt autonomic regulation.

Extensive cerebellar injury emerged in HF subjects; this injury was predominantly on the right side and was prominent in the vermis. Cerebellar regions, including the cerebellar cortices and deep nuclei, typically are associated with motor regulation. However, the cerebellar cortices, especially the vermis (Moruzzi, 1950), also play autonomic and chemoreceptor roles as well as respiratory motor regulation (Lutherer and Williams, 1986; Holmes et al., 2002). Cerebellar injury is typically accompanied by breathing disorders (Chokroverty et al., 1984; Waters et al., 1998); cerebellar structures are activated immediately on resumption of breathing after apnea (Lutherer and Williams, 1986) and induce compensatory actions to dampen extreme blood pressure changes (Lutherer et al., 1983). Both the cerebellar cortex and the fastigial deep nuclei respond significantly to autonomic challenges in adult control subjects examined with functional MRI procedures (Woo et al., 2005, 2007); both responses are diminished and distorted in HF subjects (Woo et al., 2005, 2007).

Cerebellar Purkinje cells project to cerebellar deep nuclei, and these deep nuclei project to medullary sympathetic nervous system regulatory regions (Yates and Bronstein, 2005). Injury to the cerebellar cortices and deep nuclei is suspected of contributing to the impaired blood pressure control and especially to the incidence of orthostatic hypotension and poor recovery from provoked elevations in blood pressure frequently found in HF patients (Lutherer et al., 1983). Because the cerebellar deep fastigial nuclei are sensitive to CO_2 (Xu et al., 2001), injury to those nuclei may alter chemosensitivity, enhancing the potential for the appearance of Cheyne-Stokes breathing patterns, a condition that results from altered chemosensitivity, which is common in HF (Woo et al., 2003).

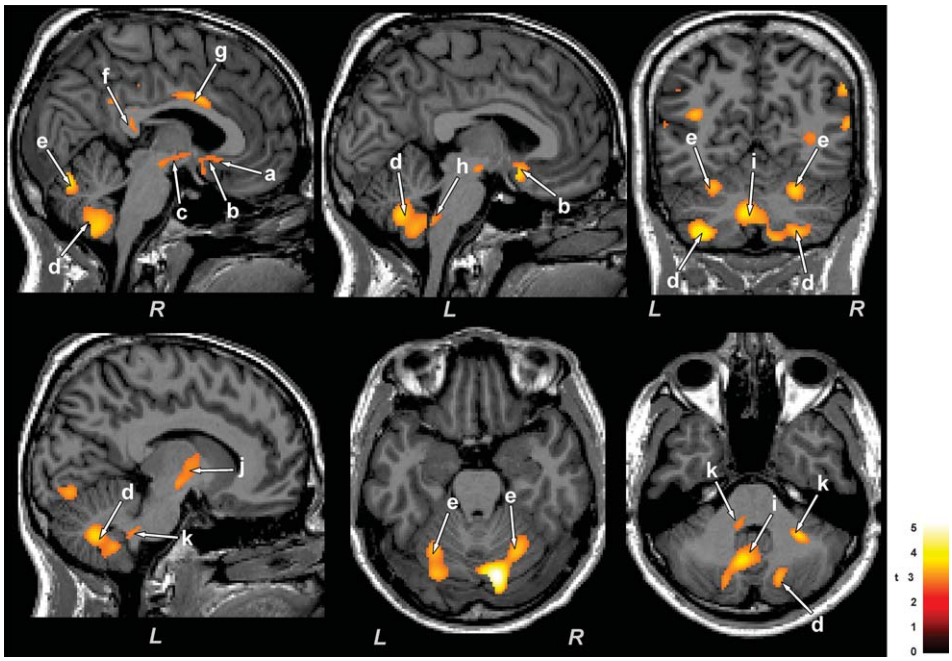

Fig. 3. Brain regions with increased MD values in HF compared with control subjects. Brain sites with increased MD values in HF subjects include the genu of cingulate (a), extending to hypothalamus (b), ventrolateral tegmental area (c), cerebellar vermis (e), cerebellar cortices (d), extending to deep nuclei (i), raphe extending to nucleus of the solitary tract (h), and inferior cerebellar peduncles (k). Figure conventions are the same as for Figure 2.

Cognitive, Mood, Dyspnea, and Language Control Regions and Brain Injury

HF patients show a variety of cognitive issues, including memory deficits (Zuccala et al., 2005; Woo et al., 2009). Brain regions that regulate cognitive, behavioral, and planning functions include the hippocampus, anterior thalamus, fornix, mammillary bodies, caudate nuclei, putamen, cerebellum, and frontal cortices; the majority of these areas showed tissue injury in HF. The hippocampus sends information to the mammillary bodies via the fornix (Aggleton et al., 2005), and mammillary bodies send efferent signals to the anterior thalamus and more caudal structures (Shibata, 1992). Both the hippocampus and the anterior thalamus showed injury here; the mammillary bodies and fornix fibers showed damage in an earlier study that evaluated injury based on high-resolution anatomical MRI procedures (Kumar et al., 2009). The caudate nuclei send and receive information to multiple brain sites, including thalamic and frontal regions, via the putamen (all these areas showed tissue injury here) and contribute to higher order cognitive and affective functions (Naismith et al., 2002). Lesion studies show that caudate and putamen damage can result in behavioral and learning deficits, and, similarly, deficits can be reproduced from damage in the frontal sites (Naismith et al., 2002; Ell et al., 2006). Cerebellar regions send and receive information from rostral brain structures and also serve cognitive and affective brain functions (Haines and Dietrichs, 1984). Thus, damage found here in cognitive, behavioral, and planning regulatory regions in HF patients may contribute to symptoms found in the syndrome.

Other common characteristics of HF patients include a high incidence of depression and elevated signs of dyspnea (Jiang et al., 2007). Several brain regions, including the insula, cingulate, hippocampus, ventral medial prefrontal cortex, and cerebellar areas, are damaged in subjects with depression without HF, and most of these sites are also injured in HF patients (Haines and Dietrichs, 1984; Agid et al., 2003; Keedwell et al., 2005). Dyspnea, the perception of breathlessness, is common in HF patients and appears to be regulated by the cingulate, insular, and cerebellar areas (Banzett et al., 2000; Peiffer et al., 2001). Those sites were injured here, possibly contributing to dyspneic feelings and reduced feelings of pleasure, both commonly found in HF patients.

Both the mid- and the posterior corpus callosum showed tissue injury in HF subjects. Corpus callosum fibers connect the two hemispheres and play significant roles in communication and integration of sensory and other information between cortical sites. Midcorpus callosum fibers connect to language areas, with injured fibers contributing to expressive aphasia (Friederici et al., 2007), whereas posterior portions of the corpus callosum connect to primary/secondary visual regions, with damage contributing to visual issues (Rudge and Warrington, 1991), as frequently anecdotally reported in HF patients. Agenesis of the corpus

callosum in humans without HF leads to difficulties in communication and language (Friederici et al., 2007), and lesions in the posterior corpus callosum introduce visual impairments (Rudge and Warrington, 1991).

Potential Pathological Mechanisms

Although the precise pathological mechanisms that contribute to brain tissue changes to autonomic, respiratory, motor, mood, and cognitive control sites are unclear, several possibilities exist. HF patients show compromised cerebral perfusion resulting from low cardiac output, a primary characteristic of the condition, as well as hypoxic/ischemic processes that accompany sleep-disordered breathing (HF patients show both obstructive and central sleep apnea; Harper et al., 2014). Both aspects may contribute to brain changes in the condition. However, these conditions should show generalized hypoxia/ischemia-induced brain changes, but HF patients show region-specific and localized tissue damage.

Another process contributing to damage may be the occurrence of initial injury in autonomic control sites, including the NTS, insular cortices, and cerebellar areas, from stroke, maldevelopment, or infection. Initial injury to NTS and to other autonomic control sites may compromise vascular activity, with impaired vascular responses leading to altered perfusion, introducing secondary injury in limbic and other rostral brain areas; damage in these latter areas is commonly found in HF patients and also is described in the current study.

The increased global and regional MD values in HF patients would suggest a chronic, rather than an acute, process. Any of the hypoxic or ischemic pathological processes would require a period of time to develop; HF is a slowly emerging condition, typically requiring several years to manifest symptoms. The slow emergence of characteristics offers the potential for intervention before more-extreme pathological characteristics emerge.

Limitations

Limitations of this study include inclusion of only HF patients classified as NYHA functional class II. We excluded HF patients with NYHA III and IV because HF patients with those categories have difficulty laying supine in the MRI machine for long periods; thus, our results should not be generalized to other NYHA functional classes. Other limitations of this study include insufficient power (small sample) to examine differences among clinically relevant subgroups of HF patients, recruitment of all HF subjects from a single referral center, and treatment of HF subjects with background guideline-directed medical therapies.

CONCLUSIONS

MD measures show increased global and regional values in multiple brain areas in HF compared with control subjects, indicating chronic tissue changes in those sites. These areas include autonomic and motor regulatory sites, including the insular cortices, hypothalamus, cerebellar cortices and deep nuclei, and other brain regions, including the limbic, basal ganglia, thalamic, frontal, NTS, and occipital regions that control cognitive and mood functions. The pathological mechanisms contributing to chronic tissue changes in HF may result from a combination of ischemic and hypoxic processes accompanying the syndrome.

ACKNOWLEDGMENTS

The authors thank Mrs. Rebecca Harper, Mr. Edwin Valladares, and Drs. Rebecca Cross and Stacy Serber for assistance with data collection. The authors have no conflicts of interest.

REFERENCES

Aggleton JP, Vann SD, Saunders RC. 2005. Projections from the hippocampal region to the mammillary bodies in macaque monkeys. Eur J Neurosci 22:2519–2530.

Agid R, Levin T, Gomori JM, Lerer B, Bonne O. 2003. T2-weighted image hyperintensities in major depression: focus on the basal ganglia. Int J Neuropsychopharmacol 6:215–224.

Ahlhelm F, Schneider G, Backens M, Reith W, Hagen T. 2002. Time course of the apparent diffusion coefficient after cerebral infarction. Eur Radiol 12:2322–2329.

Ashburner J, Friston KJ. 2005. Unified segmentation. Neuroimage 26: 839–851.

Banzett RB, Mulnier HE, Murphy K, Rosen SD, Wise RJ, Adams L. 2000. Breathlessness in humans activates insular cortex. Neuroreport 11:2117–2120.

Basser PJ, Pierpaoli C. 1996. Microstructural and physiological features of tissues elucidated by quantitative-diffusion-tensor MRI. J Magn Reson B 111:209–219.

Basser PJ, Pierpaoli C. 1998. A simplified method to measure the diffusion tensor from seven MR images. Magn Reson Med 39:928–934.

Cechetto DF, Saper CB. 1987. Evidence for a viscerotopic sensory representation in the cortex and thalamus in the rat. J Comp Neurol 262: 27–45.

Cechetto DF, Chen SJ. 1990. Subcortical sites mediating sympathetic responses from insular cortex in rats. Am J Physiol 258:R245–R255.

Chokroverty S, Sachdeo R, Masdeu J. 1984. Autonomic dysfunction and sleep apnea in olivopontocerebellar degeneration. Arch Neurol 41: 926–931.

Critchley HD, Mathias CJ, Josephs O, O'Doherty J, Zanini S, Dewar BK, Cipolotti L, Shallice T, Dolan RJ. 2003. Human cingulate cortex and autonomic control: converging neuroimaging and clinical evidence. Brain 126:2139–2152.

Dirnagl U, Iadecola C, Moskowitz MA. 1999. Pathobiology of ischaemic stroke: an integrated view. Trends Neurosci 22:391–397.

Ell SW, Marchant NL, Ivry RB. 2006. Focal putamen lesions impair learning in rule-based, but not information-integration categorization tasks. Neuropsychologia 44:1737–1751.

Friederici AD, von Cramon DY, Kotz SA. 2007. Role of the corpus callosum in speech comprehension: interfacing syntax and prosody. Neuron 53:135–145.

Haines DE, Dietrichs E. 1984. An HRP study of hypothalamo-cerebellar and cerebello-hypothalamic connections in squirrel monkey (*Saimiri sciureus*). J Comp Neurol 229:559–575.

Harper RM, Kumar R, Macey PM, Woo MA, Ogren JA. 2014. Affective brain areas and sleep-disordered breathing. Prog Brain Res 209:275–293.

Holmes MJ, Cotter LA, Arendt HE, Cass SP, Yates BJ. 2002. Effects of lesions of the caudal cerebellar vermis on cardiovascular regulation in awake cats. Brain Res 938:62–72.

Hossmann KA. 1971. Cortical steady potential, impedance and excitability changes during and after total ischemia of cat brain. Exp Neurol 32: 163–175.

Jiang H, van Zijl PC, Kim J, Pearlson GD, Mori S. 2006. DtiStudio: resource program for diffusion tensor computation and fiber bundle tracking. Comput Methods Programs Biomed 81:106–116.

Jiang W, Kuchibhatla M, Clary GL, Cuffe MS, Christopher EJ, Alexander JD, Califf RM, Krishnan RR, O'Connor CM. 2007. Relationship between depressive symptoms and long-term mortality in patients with heart failure. Am Heart J 154:102–108.

Keedwell PA, Andrew C, Williams SC, Brammer MJ, Phillips ML. 2005. The neural correlates of anhedonia in major depressive disorder. Biol Psychiatry 58:843–853.

King AB, Menon RS, Hachinski V, Cechetto DF. 1999. Human forebrain activation by visceral stimuli. J Comp Neurol 413:572–582.

Kumar R, Woo MA, Birrer BV, Macey PM, Fonarow GC, Hamilton MA, Harper RM. 2009. Mammillary bodies and fornix fibers are injured in heart failure. Neurobiol Dis 33:236–242.

Kumar R, Woo MA, Macey PM, Fonarow GC, Hamilton MA, Harper RM. 2011. Brain axonal and myelin evaluation in heart failure. J Neurol Sci 307:106–113.

Le Bihan D, Moonen CT, van Zijl PC, Pekar J, DesPres D. 1991. Measuring random microscopic motion of water in tissues with MR imaging: a cat brain study. J Comput Assist Tomogr 15:19–25.

Le Bihan D, Mangin JF, Poupon C, Clark CA, Pappata S, Molko N, Chabriat H. 2001. Diffusion tensor imaging: concepts and applications. J Magn Reson Imaging 13:534–546.

Lutherer LO, Williams JL. 1986. Stimulating fastigial nucleus pressor region elicits patterned respiratory responses. Am J Physiol 250:R418–R426.

Lutherer LO, Lutherer BC, Dormer KJ, Janssen HF, Barnes CD. 1983. Bilateral lesions of the fastigial nucleus prevent the recovery of blood pressure following hypotension induced by hemorrhage or administration of endotoxin. Brain Res 269:251–257.

Matsumoto K, Lo EH, Pierce AR, Wei H, Garrido L, Kowall NW. 1995. Role of vasogenic edema and tissue cavitation in ischemic evolution on diffusion-weighted imaging: comparison with multiparameter MR and immunohistochemistry. Am J Neuroradiol 16:1107–1115.

Menzler K, Belke M, Wehrmann E, Krakow K, Lengler U, Jansen A, Hamer HM, Oertel WH, Rosenow F, Knake S. 2011. Men and women are different: diffusion tensor imaging reveals sexual dimorphism in the microstructure of the thalamus, corpus callosum, and cingulum. Neuroimage 54:2557–2562.

Moruzzi G. 1950. The cerebellar influence in the autonomic sphere. In: Thomas CC, editor. Problems in cerebellar physiology. Springfield, IL: Literary Licensing. p 74–96.

Naismith S, Hickie I, Ward PB, Turner K, Scott E, Little C, Mitchell P, Wilhelm K, Parker G. 2002. Caudate nucleus volumes and genetic determinants of homocysteine metabolism in the prediction of psychomotor speed in older persons with depression. Am J Psychiatry 159: 2096–2098.

O'Dell TJ, Huang PL, Dawson TM, Dinerman JL, Snyder SH, Kandel ER, Fishman MC. 1994. Endothelial NOS and the blockade of LTP by NOS inhibitors in mice lacking neuronal NOS. Science 265:542–546.

Oppenheimer SM, Gelb A, Girvin JP, Hachinski VC. 1992. Cardiovascular effects of human insular cortex stimulation. Neurology 42:1727–1732.

Oppenheimer SM, Kedem G, Martin WM. 1996. Left-insular cortex lesions perturb cardiac autonomic tone in humans. Clin Auton Res 6: 131–140.

Peiffer C, Poline JB, Thivard L, Aubier M, Samson Y. 2001. Neural substrates for the perception of acutely induced dyspnea. Am J Respir Crit Care Med 163:951–957.

Radford MJ, Arnold JM, Bennett SJ, Cinquegrani MP, Cleland JG, Havranek EP, Heidenreich PA, Rutherford JD, Spertus JA, Stevenson LW, Goff DC, Grover FL, Malenka DJ, Peterson ED, Redberg RF, American College of Cardiology, American Heart Association Task Force on Clinical Data Standards, American College of Chest Physicians, International Society for Heart and Lung Transplantation, Heart Failure Society of America. 2005. ACC/AHA key data elements and definitions for measuring the clinical management and outcomes of patients with chronic heart failure: a report of the American College of Cardiology/American Heart Association Task Force on Clinical Data Standards (Writing Committee to Develop Heart Failure Clinical Data Standards): developed in collaboration with the American College of Chest Physicians and the International Society for Heart and Lung Transplantation: endorsed by the Heart Failure Society of America. Circulation 112:1888–1916.

Rorden C, Karnath HO, Bonilha L. 2007. Improving lesion-symptom mapping. J Cogn Neurosci 19:1081–1088.

Rudge P, Warrington EK. 1991. Selective impairment of memory and visual perception in splenial tumours. Brain 114:349–360.

Saper CB. 1982. Convergence of autonomic and limbic connections in the insular cortex of the rat. J Comp Neurol 210:163–173.

Shibata H. 1992. Topographic organization of subcortical projections to the anterior thalamic nuclei in the rat. J Comp Neurol 323:117–127.

Shipley MT. 1982. Insular cortex projection to the nucleus of the solitary tract and brainstem visceromotor regions in the mouse. Brain Res Bull 8:139–148.

Waters KA, Forbes P, Morielli A, Hum C, O'Gorman AM, Vernet O, Davis GM, Tewfik TL, Ducharme FM, Brouillette RT. 1998. Sleep-disordered breathing in children with myelomeningocele. J Pediatr 132:672–681.

Westerhausen R, Kompus K, Dramsdahl M, Falkenberg LE, Gruner R, Hjelmervik H, Specht K, Plessen K, Hugdahl K. 2011. A critical reexamination of sexual dimorphism in the corpus callosum microstructure. Neuroimage 56:874–880.

Woo MA, Macey PM, Fonarow GC, Hamilton MA, Harper RM. 2003. Regional brain gray matter loss in heart failure. J Appl Physiol 95:677–684.

Woo MA, Macey PM, Keens PT, Kumar R, Fonarow GC, Hamilton MA, Harper RM. 2005. Functional abnormalities in brain areas that mediate autonomic nervous system control in advanced heart failure. J Card Fail 11:437–446.

Woo MA, Macey PM, Keens PT, Kumar R, Fonarow GC, Hamilton MA, Harper RM. 2007. Aberrant central nervous system responses to the Valsalva maneuver in heart failure. Congest Heart Fail 13:29–35.

Woo MA, Kumar R, Macey PM, Fonarow GC, Harper RM. 2009. Brain injury in autonomic, emotional, and cognitive regulatory areas in patients with heart failure. J Card Fail 15:214–223.

Xu F, Zhang Z, Frazier DT. 2001. Microinjection of acetazolamide into the fastigial nucleus augments respiratory output in the rat. J Appl Physiol 91:2342–2350.

Yates BJ, Bronstein AM. 2005. The effects of vestibular system lesions on autonomic regulation: observations, mechanisms, and clinical implications. J Vestib Res 15:119–129.

Zhang ZH, Rashba S, Oppenheimer SM. 1998. Insular cortex lesions alter baroreceptor sensitivity in the urethane-anesthetized rat. Brain Res 813:73–81.

Zuccala G, Marzetti E, Cesari M, Lo Monaco MR, Antonica L, Cocchi A, Carbonin P, Bernabei R. 2005. Correlates of cognitive impairment among patients with heart failure: results of a multicenter survey. Am J Med 118:496–502.